

Chladni Figures Revisited Based on Nanomechanics

M. Dorrestijn,^{1,2} A. Bietsch,^{1,2,*} T. Açıkalın,³ A. Raman,³ M. Hegner,¹ E. Meyer,^{1,†} and Ch. Gerber¹

¹National Center of Competence in Research on Nanoscale Science, Institute of Physics, University of Basel, Basel, Switzerland

²IBM Research, Zurich Research Laboratory, Rüschlikon, Switzerland

³School of Mechanical Engineering and the Birck Nanotechnology Center, Purdue University, West Lafayette, Indiana, USA

(Received 20 June 2006; published 8 January 2007)

Chladni patterns based on nanomechanics in the microfluidic environment are presented. In contrast with the macroscopic observations in the gaseous environment, nanoparticles are found to move to the nodes, whereas micron-sized particles move to the antinodes of the vibrating interface. This opens the door to size-based sorting of particles in microfluidic systems, and to highly parallel and controlled assembly of biosensors and nanoelectronic circuits.

DOI: [10.1103/PhysRevLett.98.026102](https://doi.org/10.1103/PhysRevLett.98.026102)

PACS numbers: 81.16.Rf, 47.85.-g

In recent years, there has been increasing interest in the positioning of micro- and nanoparticles on surfaces. Applications include biosensors [1,2] and molecular electronics [3,4]. For automated patterning of particles, existing methods are either slow (e.g., dip-pen lithography [1,5]) or require prefabricated patterns (e.g., by electrostatic positioning [6] or by successive self-assembly, transfer, and integration [7]). Moreover, the sorting of differently sized particles, organelles, and cells in microfluidic networks is important for many biological and medical applications. Purely size-based sorting would offer the greatest control, but an automated method appears to be inexistent. Current methods sort particles based on density and size (size-selective precipitation [8], ratchets [9] and the “Brazil nut effect” [10,11]), surface properties and size (high-performance liquid chromatography [12]), charge and size (gel electrophoresis [13]), dielectric constant and size (dielectrophoresis [14,15]), and acoustic impedance and size (ultrasonic separation [16]).

In 1787, the German physicist Chladni showed how sand particles could be made to self-organize into symmetrical patterns [17]. Upon excitation of a metal plate with a violin bow, the sand on it would group along the nodal lines. The patterns, which vary with different modes of resonance, were named Chladni figures. Chladni also reported how fine particles (fine shavings from the hairs of his violin bow) would move in the opposite direction, to the antinodes. The latter behavior was found by Faraday [18] to be due to induced air currents, now known as acoustic streaming.

Acoustic streaming is a steady circulatory flow that can be generated in oscillating fluids. The oscillation can be driven by a sound field in a compressible medium (“quartz wind”) or by an oscillating surface in a viscous medium (“boundary streaming”) [19,20]. The latter results from the convective inertia term of the Navier-Stokes equation, which has a nonzero time average. Boundary streaming near oscillating beam structures has recently gained interest in the context of air cooling for portable electronics devices [21,22].

In this Letter, microscale Chladni figures are presented for the first time. It is shown that nanoscale oscillations of cantilever beams in liquid drive particles initially resting on the surface either to the nodes or to the antinodes, depending on their size. Similar to Faraday’s findings, the size dependency results from boundary streaming. However, the size dependency is found to be inverted at small scales.

The experiments were performed in a polymethylmethacrylate microfluidic cell (100 μL , distance between glass cover and cantilevers 1.4 ± 0.2 mm) filled with water, and observed using dark-field microscopy. Silicon cantilever arrays of $560 \times 100 \times 7$ μm^3 (fabricated by KOH and deep reactive ion etching at the IBM Zurich Research Laboratory) were mounted directly on top of a piezoelectric element inside the cell [23]. Arrays of cantilevers were used to improve the statistical significance of the observed patterns. The resonance frequencies and amplitudes of the cantilevers were determined in liquid by laser beam deflection [24]. Thiol-functionalized polystyrene beads (Merck-Estapor, France) with a ferrite core (iron (III) oxide) were size selected by centrifugation to obtain batches of 4 ± 1 μm (microbeads) or 0.5 ± 0.3 μm (nanobeads), as determined by scanning electron microscopy [(SEM), see Fig. 1]. The observed diameter of the ferrite core was a fraction 0.54 ± 0.06 of the total bead diameter, giving a density of 1.7 ± 0.2 g/cm^3 . The microfluidic cell was filled with homogeneous suspensions of micro- or nanobeads, which settled by gravity within 20 min or 3 h, respectively, (settling velocities 6 $\mu\text{m}/\text{s}$ and 100 nm/s). Subsequent excitation of the cantilevers was performed at sequential resonance modes.

The resonance frequencies of the first six resonance modes ranged from 12 kHz to 1.3 MHz. The corresponding vibration amplitudes ranged from 400 down to 8 nm. For modes 3–6, 4- μm beads were seen to move towards the antinodes of vibration, forming well-defined groups within 20–25 s [25]. The positions of the antinodes were confirmed by direct observation of the locations of edge vortices containing trapped beads (this phenomenon has been

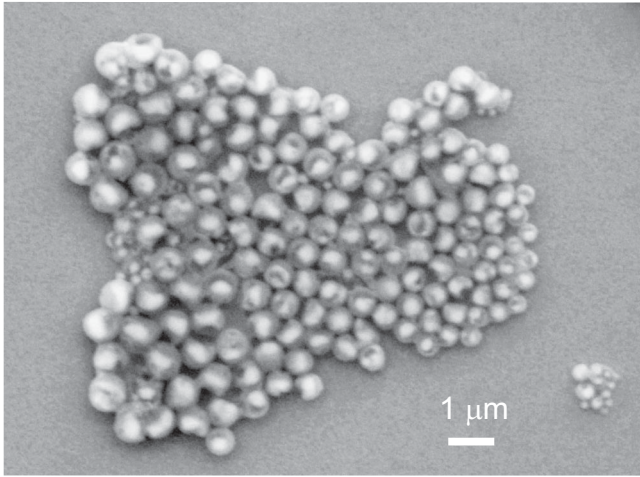


FIG. 1. SEM image of the nanobeads. The observed diameter is $0.5 \pm 0.3 \mu\text{m}$. The image was recorded without gold coating on the beads, making the ferrite cores visible.

demonstrated for liquid [26] and for air [22]). Groups could be repositioned by switching to a neighboring resonance mode, as demonstrated in Fig. 2(a) (video available online [27]).

The $0.5\text{-}\mu\text{m}$ beads, however, moved towards the nodes, as shown in Fig. 2(c). Pattern formation took significantly longer, namely, 13–17 min. The opposite directionality of differently sized beads can be explained by assuming that the beads are dragged by boundary streaming. In air, the classical Chladni figures formed when sand particles bounced off the antinodes and came to rest on the nodes. Only for fine powder were the lateral inertia forces dominated by the viscous drag of boundary streaming towards the antinodes. In microfluidics, both small and large particles follow the direction of the near field hydrodynamics; gravitational forces do not play a central role in pattern formation. An analytical model of the boundary streaming in water was obtained by solving the Navier-Stokes equation near an infinitely wide, oscillating beam, as published elsewhere [21]. Figure 3 shows stream lines of the water

near the cantilever surface for the 4th resonance mode. The schematic micro- and nanobeads show how the particle size determines which flow direction of boundary streaming will be followed. The flattened vortices (of cross-section $2 \times 80 \mu\text{m}^2$) are called the inner circulations. The forces on the beads were calculated by integrating the Stokes drag force over the height of the sphere, using

$$F_D = 3\pi\eta \int_0^D u(h)dh, \quad (1)$$

where u is the horizontal component of the water velocity, h is the distance from the cantilever surface, D is the bead diameter, and η the viscosity. A critical bead diameter was obtained by solving Eq. (1) ($F_D = 0$); this diameter is equal to the height of the inner circulations. This height is frequency dependent, and the resulting graph is shown in Fig. 4. A fit was made using the conventional formula for the Stokes boundary layer thickness δ [28]

$$\delta \approx \sqrt{\frac{2\nu}{\omega}}, \quad (2)$$

where ω is the radial frequency of oscillation and ν the kinematic viscosity of the medium. A multiplicative fitting constant of 2.8 was found. The geometrical interpretation is that the distance from the circulation center to the surface is close to δ , as indicated in Fig. 3. The reason for this is that the boundary streaming is driven by the oscillatory flow within the Stokes boundary layer. From Fig. 4 it can be seen that the nanobeads were smaller than the critical bead diameter in the entire frequency range, whereas the microbeads were larger than the critical size above 100 kHz. In sorting applications, smaller critical sizes are achieved at higher frequencies while controlling the node-node distance by the choice of the beam thickness. For media of higher viscosity, the critical diameter increases. In vacuum, it could be that the nanobeads enter the superlubricity regime [29,30].

Some beads on the cantilever were seen to fall off the surface. The lost fraction can be reduced by making the

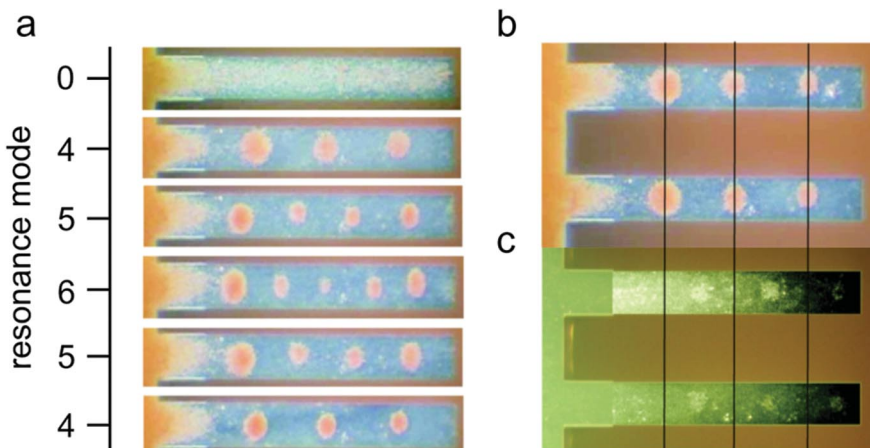


FIG. 2 (color). (a) Time evolution of microbead patterns on one cantilever (length $560 \mu\text{m}$) upon sequential excitation of different resonance modes (no excitation, 4th, 5th, 6th, 5th, and 4th mode). The total time lapse was 2 min. (b) Patterns formed on two adjacent cantilevers by excitation of the 4th mode. Microbeads ($4 \mu\text{m}$) group on the antinodes, whereas nanobeads ($0.5 \mu\text{m}$) group on the nodes (c). Vertical lines mark the positions of the antinodes.

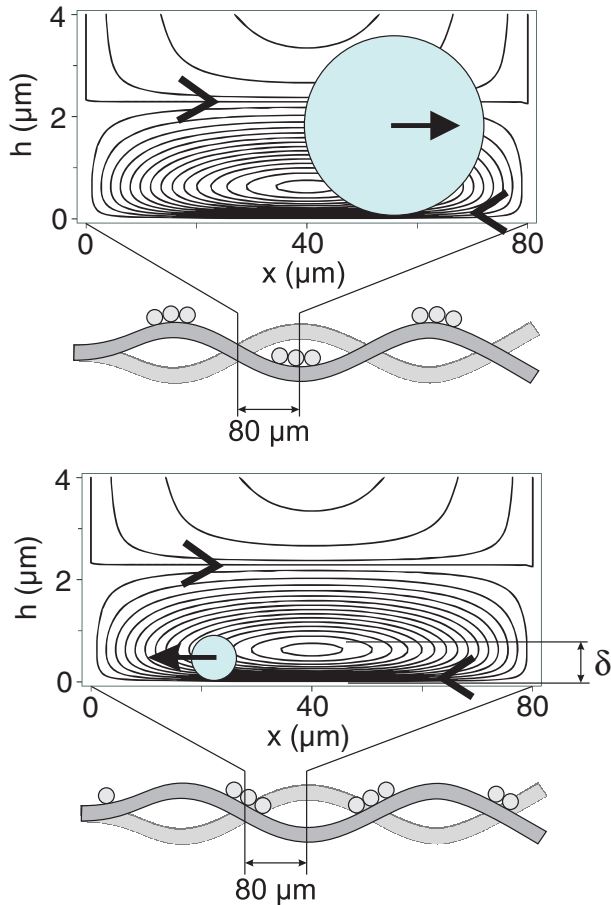


FIG. 3 (color). Calculated stream lines for water near the surface of an oscillating microcantilever. Shown is the 4th resonance mode, for which the quarter wavelength was $80 \mu\text{m}$ and the frequency 500 kHz . The cantilever was modeled as being infinitely wide and long. The x axis coincides with the cantilever axis, and the h axis extends into the bulk liquid. Differently sized beads (light blue circles) are dragged in opposite directions. The height of the Stokes boundary layer thickness is indicated by δ .

cantilevers wider or by using membranes. The reader is referred to the additional video material [27], where it is evident that the majority of the beads remained on the cantilever even after cycling through different resonances 5 times.

The beads interacted with the cantilever surface by weak forces. Two observations suggest that while grouping on the oscillating surface, the microbeads bounced slightly, whereas the nanobeads rolled or hopped intermittently. During intermittent hopping, beads remain bound to the surface until released by thermal energy. Before resorbing, they migrate in the direction of the streaming flow. The first observation is that the nanobeads followed the narrow stream closest to the surface. This indicates that they were held close to the surface, whereas the simple Boltzmann height distribution [Eq. (3)] predicts an average bead height $\langle h \rangle$ of $9 \mu\text{m}$ from

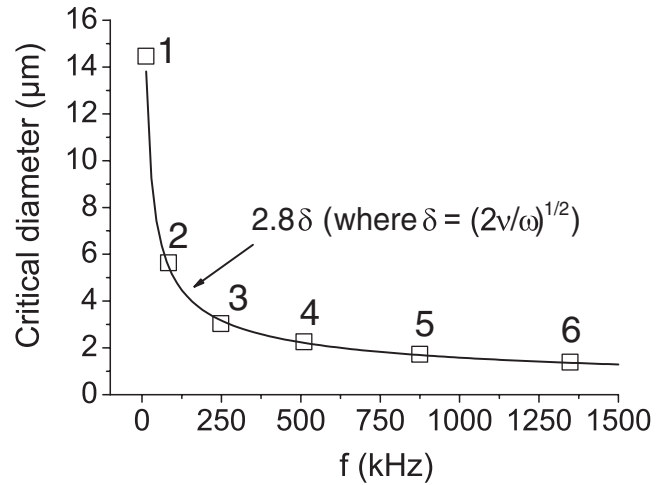


FIG. 4. Critical bead diameter vs frequency, which indicates the critical size for particle sorting (squares). The horizontal force of boundary streaming acting on a spherical particle was calculated from the integrated Stokes drag force. The continuous line corresponds to the Stokes boundary layer thickness δ [Eq. (2)] multiplied by a fitting factor of 2.8.

$$\frac{n}{n_o} = \exp\left(-\frac{m_n g h}{kT}\right) \Rightarrow \langle h \rangle = kT/(m_n g), \quad (3)$$

where k is Boltzmann's constant, T the temperature, m_n the buoyant mass of a nanobead, and g the acceleration due to gravity. The second observation is that the $0.5\text{-}\mu\text{m}$ nanobeads moved 30–50 times slower along the cantilever surface than the $4\text{-}\mu\text{m}$ microbeads did. This suggests that the nanobeads were slowed down by interaction with the surface. For the $4\text{-}\mu\text{m}$ microbeads, on the other hand, the surface interactions were conceivably dominated by the vertical momentum of the beads. The surface transferred a 500 times larger kinetic energy to the microbeads than to the nanobeads, owing to the difference in their mass [31]. The propagation velocity of the nanobeads might be enhanced by varying the surface chemistry. The chemical interaction can be tuned by adapting the chemical groups [32,33] and controlling the pH .

In conclusion, inverted Chladni figures were formed on oscillating microcantilevers in the aqueous environment. Microbeads were found to collect on the antinodes, whereas nanobeads moved towards the nodes of vibration. This demonstrates the inverse size-dependent directionality as compared with Chladni's observations owing to induced streaming of the liquid. The applied analytical model for boundary streaming predicts a critical, frequency-dependent bead diameter at which beads reverse direction, which was experimentally observed. The demonstration of Chladni figures in microfluidics presented here opens the door to highly parallel, directed assembly and to size-based sorting or size-dependent manipulation of particles, organelles, or cells. In sorting applications, particles on the nodes and antinodes could be transported

along orthogonal paths such as dielectrophoretic paths [15]. Combined with time segregation, this allows for additional selection on chemical composition of the separated objects. The propagation times can be tuned by the choice of surface chemistry and appropriate buffering of the solution. Sorting of more than two different sizes is possible by using harp-shaped cantilever arrays and sweeping through the consecutive resonance frequencies. In patterning applications, the use of membrane structures instead of cantilevers will offer a larger variety of patterns. Grouped particles can be fixed using laser curing, photopolymerization or selective electroless deposition on metal [34] or polymer [35]. After fixation, the liquid is removed and the patterns are transferred from the membrane to a chip surface by nanotransfer printing (nTP) [7,36], leading to controlled, multistep assembly of biotechnological sensors or nanoelectronic circuits.

We gratefully thank U. Dürig, H.P. Lang, R. Lindermann, M. Stöhr, and A. Baratoff for fruitful discussions. We also thank U. Drechsler for helpful SEM work. Funding was provided by the National Center of Competence in Research on Nanoscale Science. The continuous support of R. Allenspach and P.F. Seidler (IBM Zurich Research Laboratory, Switzerland) is gratefully acknowledged.

*Present address: OC Oerlikon Balzers Ltd., Balzers, Liechtenstein.

†Corresponding author.

Electronic address: ernst.meyer@unibas.ch

- [1] K.B. Lee, S.J. Park, C.A. Mirkin, J.C. Smith, and M. Mrksich, *Science* **295**, 1702 (2002).
- [2] M.S. Wilson and W. Nie, *Anal. Chem.* **78**, 2507 (2006).
- [3] K. Keren, R.S. Berman, E. Buchstab, U. Sivan, and E. Braun, *Science* **302**, 1380 (2003).
- [4] J.M. Seminario, *Nat. Mater.* **4**, 111 (2005).
- [5] M. Zhang, D. Bullen, S.W. Chung, S. Hong, K.S. Ryu, Z. Fan, C.A. Mirkin, and C. Liu, *Nanotechnology* **13**, 212 (2002).
- [6] S.W. Lee and R. Bashir, *Appl. Phys. Lett.* **83**, 3833 (2003).
- [7] T. Kraus, L. Malaquin, E. Delamarche, H. Schmid, N.D. Spencer, and H. Wolf, *Adv. Mater.* **17**, 2438 (2005).
- [8] C.B. Murray, D.J. Norris, and M.G. Bawendi, *J. Am. Chem. Soc.* **115**, 8706 (1993).
- [9] A. Ros, R. Eichhorn, J. Regtmeier, T. Duong, P. Reimann, and D. Anselmetti, *Nature (London)* **436**, 928 (2005).
- [10] A. Rosato, K.J. Strandburg, F. Prinz, and R.H. Swendsen, *Phys. Rev. Lett.* **58**, 1038 (1987).
- [11] D.A. Huerta and J.C. Ruiz-Suárez, *Phys. Rev. Lett.* **92**, 114301 (2004).
- [12] Ch.-H. Fischer, H. Weller, L. Katsikas, and A. Henglein, *Langmuir* **5**, 429 (1989).
- [13] A. Eychmüller, L. Katsikas, and H. Weller, *Langmuir* **6**, 1605 (1990).
- [14] N.G. Green and H. Morgan, *J. Phys. D* **31**, L25 (1998).
- [15] H. Li and R. Bashir, *Sensors and Actuators B (Chemical)* **86**, 215 (2002).
- [16] M.K. Araz, C.H. Lee, and A. Lal, *Ultrasonics Symposium (IEEE, New York, 2003)*, p. 1066.
- [17] E.F.F. Chladni, *Entdeckungen über die Theorie des Klanges* (Breitkopf und Härtel, Leipzig, 1787).
- [18] M. Faraday, *Phil. Trans. R. Soc. London* **121**, 299 (1831).
- [19] W.L. Nyborg, in *Nonlinear Acoustics*, edited by M.F. Hamilton and D.T. Blackstock (Academic, San Diego, 1998), Chap. 7, p. 207.
- [20] N. Riley, *Annu. Rev. Fluid Mech.* **33**, 43 (2001).
- [21] T. Açıkalın, A. Raman, and S.V. Garimella, *J. Acoust. Soc. Am.* **114**, 1785 (2003).
- [22] R.J. Linderman, O. Nilsen, and V.M. Bright, *Sens. Actuators A, Phys.* **118**, 162 (2005).
- [23] T. Braun, V. Barwich, M.K. Ghatkesar, A.H. Bredekamp, Ch. Gerber, M. Hegner, and H.P. Lang, *Phys. Rev. E* **72**, 031907 (2005).
- [24] G. Meyer and N.M. Amer, *Appl. Phys. Lett.* **53**, 1045 (1988).
- [25] For the second mode, edge vortices dragged the 4- μm beads off the edges of the cantilever before grouping could be observed. Edge vortices were more pronounced for modes with larger node-node distances (lower mode numbers).
- [26] A. Sathaye and A. Lal, in *Ultrasonics Symposium (IEEE, New York, 2001)*, p. 641.
- [27] See EPAPS Document No. E-PRLTAO-98-076701 for videos showing the formation of Chladni figures using 4- μm beads. For more information on EPAPS, see <http://www.aip.org/pubservs/epaps.html>.
- [28] G.K. Batchelor, *An Introduction to Fluid Dynamics* (Cambridge University Press, Cambridge, England, 1994), p. 354, 1st ed.
- [29] A. Socoliuc, R. Bennewitz, E. Gnecco, and E. Meyer, *Phys. Rev. Lett.* **92**, 134301 (2004).
- [30] A. Socoliuc, E. Gnecco, S. Maier, O. Pfeiffer, A. Baratoff, R. Bennewitz, and E. Meyer, *Science* **313**, 207 (2006).
- [31] For the fourth resonance mode, i.e., at 500 kHz and an amplitude of 20 nm, the kinetic energy transferred to a microbead is $\frac{1}{2}m_m v_{\text{max}}^2 = 26000$ kT. Here, $m_m = 57$ pg is the mass of a microbead and $v_{\text{max}} = 63$ mm/s the velocity amplitude of the oscillating cantilever surface. The binding energy of a single weak bond is a few kT.
- [32] M. Hegner, *Single Mol.* **1**, 139 (2000).
- [33] G.T. Hermanson, *Bioconjugate Techniques* (Academic, San Diego, 1996).
- [34] C.H. Ting and M. Paunovic, *J. Electrochem. Soc.* **136**, 456 (1989).
- [35] T.G. Vargo, J.A. Gardella, J.M. Calvert, and M.S. Chen, *Science* **262**, 1711 (1993).
- [36] S. Hur, D. Khang, C. Kocabas, and J. Rogers, *Appl. Phys. Lett.* **85**, 5730 (2004).